Meso-scale Viscoelastic Properties of Achilles Tendon Matrix Reveal Local Contributions to Tissue Mechanics

Tyler E. Blanch[1], Yu-Chang Chen[1], Jonathon L. Blank[1], Kyle H. Vining[1], and Su Chin Heo[1]
[1]University of Pennsylvania, Philadelphia, PA
tblanch@seas.upenn.edu

Disclosures: Blanch (N), Chen (N), Blank (N), Vining (N), Heo (5-4WEB Medical)

INTRODUCTION: Tendons are dense connective tissues that transmit muscle forces onto bone, facilitating efficient movement **[1]**. To achieve this, tendon relies on an anisotropic collagen matrix with high elasticity to minimize energy loss during force transfer. In the context of tendon pathologies such as tendinopathy, matrix organization and composition are significantly disrupted, leading to reduced load transmission efficiency and altered material properties **[2]**. Beyond force transmission, tendon viscoelastic properties also play a critical role in regulating resident cell behavior, including mechanotransduction and matrix synthesis. Changes in viscoelasticity can therefore influence how cells sense and remodel their microenvironment. Despite this importance, how viscoelastic properties are altered in tendon disease, and how such changes contribute to tendon degeneration, remain poorly understood. Although tendon mechanics have been widely studied at the whole-tissue level under tensile loading, bulk measurements often obscure meso-scale mechanical properties arising from extracellular matrix composition and organization **[3]**. Consequently, there is a gap in our understanding of how local viscoelastic changes at the cell level contribute to disease-associated matrix remodeling. To address this gap, we employ shear rheology on Achilles tendon biopsies to determine how viscoelastic matrix contributions are affected in the case of tendon homeostasis and disuse. Here, we present our preliminary characterization of healthy tendon tissue across multiple biological donors to establish the feasibility and reproducibility of this approach. Male animals were used in this validation phase to reduce biological variability prior to extending the study to overloaded and underloaded tendon models.

		D3.1	D3.2	D4.1	D4.2	D5.1	D5.2
3% Axial Strain	Relaxation, %	55.46	56.38	68.42	59.54	55.63	60.35
	|E*|, Mpa	170.25	91.38	124.38	62.29	122.92	105.10
	tan δ	0.0652	0.0820	0.0780	0.0930	0.0638	0.0833
6% Axial Strain	Relaxation, %	45.74	52.21	49.80	55.24	48.09	53.15
	|E*|, Mpa	284.93	143.74	240.85	103.72	200.56	165.02
	tan δ	0.0495	0.0697	0.0507	0.0784	0.0525	0.0690
	GAG content (ug/mg)	6.89	7.36	14.21	8.35	7.82	8.90

Figure 1: Table outlining results from whole-tendon tensile testing, including stress relaxation, dynamic modulus (E*), and phase shift (tan(δ)) at 3% and 6% tensile strain, and glycosaminoglycan (GAG) content assay. (n=3 biological replicates with 2 contralateral limbs each, D: donor, 1: left limb, 2: right limb).

METHODS: Left and right Achilles tendons were isolated and harvested from four 10-week-old male Sprague Dawley rats (IACUC approved). For whole-tendon testing, the hindpaw was secured in polymethylmethacrylate at 120° and the proximal tendon clamped in sandpaper grips in a 37°C 1×PBS bath. Whole-tendon tensile testing consisted of a 1 N preload, 10 cycles of preconditioning at 0.5% strain, stress relaxations at 3% and 6% grip strain, followed by frequency sweeps at 0.1, 1, 5, and 10 Hz as previously reported **[4]**. Viscoelastic properties (dynamic modulus (E*), phase shift (tan(δ)), and percent relaxation) were measured. Following tensile testing, two biopsy punches (1.5mm diameter, ~0.8 mm height) were extracted from the tendon midsubstance of each tissue. Biopsies were tested in a shear rheometer under shear and compression in a 37°C 1×PBS water bath with normal force perpendicular to fiber orientation. Rheological testing consisted of a 0.01N compressive preload followed by either (1) shear strain sweeps from 0.01% - 20% (0.00063 - 1.257rad) at 0.1Hz (n=1) or (2) shear frequency sweeps from 0.01Hz – 25Hz at 0.5% strain (0.0314rad) (n=3), shear stress relaxation at 3% strain (0.1885rad), and axial compression to 90% strain at 1% strain/sec rate for two technical replicates per tissue. Viscoelastic (shear storage modulus (G′), shear loss modulus (G″), tan(δ), and percent relaxation) and elastic (stiffness, Young's modulus) properties were measured. All remaining tendon tissue was digested in proteinase K overnight at 60°C prior to quantifying glycosaminoglycan (GAG) content using the 1,9-dimethylmethylene blue assay and chondroitin sulfate as standard. Absorbance was read at 525 and 595 nm and normalized to the tendon dry weight **[5]**.

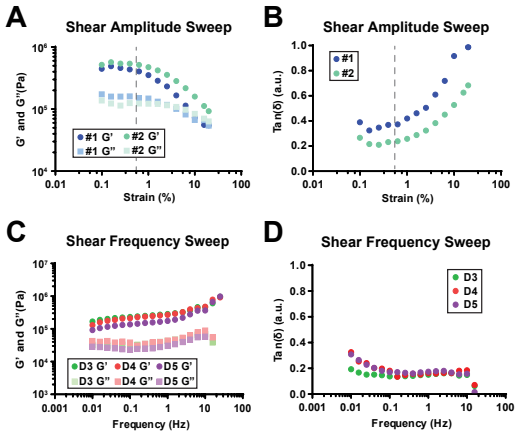

Figure 2: (A, B) Shear storage (G') and loss (G") moduli **(A)**, and phase shift (tan(δ)) **(B)**, of Achilles tendon biopsy punches measured across increasing strain magnitudes. Dashed line indicates 0.5% strain (0.0314rad). (n=2 technical replicates). **(C, D)** Shear storage (G') and loss (G") moduli **(C)**, and tan(δ) **(D)**, of Achilles tendon biopsy punches measured across increasing strain frequencies. (n=3 biological replicates, colors indicate individual donors, D: donor).

RESULTS: Whole-tendon tensile testing revealed consistent viscoelastic properties between contralateral limbs and individual donors. Tendons reached an average of 59.3% stress relaxation after 10 minutes, and phase shift (tan(δ)) averaged 0.08 (3% strain) **(Fig. 1)**. In shear, tendon biopsy punch tissues displayed linear strain behavior up to 1% strain (0.0628rad), beyond which nonlinear responses manifested **(Fig. 2A, B)**. Based on this, 0.5% strain (0.0314rad) was selected for subsequent shear measurements. Frequency sweeps of punch tissues revealed reproducible complex modulus values across samples, with tan(δ) averaging 0.18 **(Fig. 2C, D)**. Shear stress relaxation was rapid, reaching 50% relaxation within 5 minutes in all samples **(Fig. 3A)**. Axial compression of biopsy punch tissues yielded a consistent Young's modulus of 4.75 MPa (standard deviation = 0.217) averaged across biological replicates **(Fig. 3B, C)**. GAG content, measured biochemically, showed a strong correlation with stress relaxation in both tensile (3%, R^2=0.9518) and shear (R^2=0.7303) testing, linking matrix composition to viscoelastic behavior **(Fig. 1, 3)**.

DISCUSSION: Shear rheological analysis of tendon tissue provides an underexplored and complementary approach to characterizing matrix material properties, with unique sensitivity to meso-scale effects. Both whole-tendon and biopsy punch testing demonstrated consistent trends across biological samples, including relative ordering based on stress relaxation times and tan(δ). However, notable differences in the value of tan(δ) and Young's modulus between whole-tendon and biopsy-scale tests underline how bulk tissue structure can mask local mechanical properties. Meso-scale forces are particularly important to define, as they directly regulate resident tendon fibroblast mechanotransduction, gene expression, and matrix synthesis, while tissue-scale forces primarily govern macroscopic tendon function **[6]**. Disruption of local viscoelastic properties may shift tenocyte transcriptional programs away from homeostasis toward disease-associated remodeling **[7]**. Thus, shear rheology offers a powerful platform to investigate localized or heterogeneous alterations in tendon mechanics and to link matrix composition with functional outcomes in both health and disease.

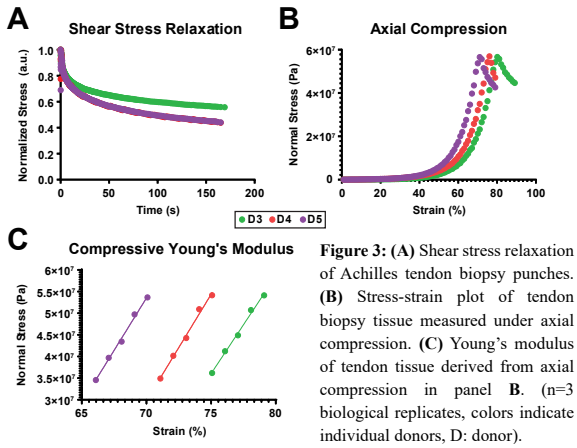

Figure 3: (A) Shear stress relaxation of Achilles tendon biopsy punches. **(B)** Stress-strain plot of tendon biopsy tissue measured under axial compression. **(C)** Young's modulus of tendon tissue derived from axial compression in panel **B**. (n=3 biological replicates, colors indicate individual donors, D: donor).

SIGNIFICANCE: This study demonstrates the use of shear rheology to characterize novel meso-scale mechanical properties of the Achilles tendon. This work provides new insight into how tendon mechanics are altered in heterogeneous conditions such as tendinopathy, with the potential to link matrix composition to disease progression.

References: **[1]** Bordoni+, *StatPearls*, 2024; **[2]** Xu+, *Clin Orth Rel Res*, 2008; **[3]** Basoli+, *Front Physio*, 2018; **[4]** Blank+, *J Physiol*, 2025; **[5]** Zheng+, *Eur Cell Mat*, 2015; **[6]** Nelson+, *Cell*, 2024; **[7]** Gardner+, *JOR*, 2012.

Acknowledgements: This work was supported by the NIH (P50 AR080581, K01 AR077087, F32 AR082671) and NSF (CMMI-1548571).